MINERALOGICAL MAGAZINE, DECEMBER 1977, VOL. 41, PP. 541–4

An unusual chlorite from Western Australia

RILEY (1975) has described a Ni-rich serpentine that occurs in drill cuttings from an ultramafic body at Woodline Well near South Windarra in Western Australia. Woodline Well is situated approximately 8 km west of the Poseidon-Western Mining Corporation nickel mine and 255 km NNE. of Kalgoorlie. The original identification as serpentine was made on the basis of the absence of a 14 Å X-ray powder diffraction line that would be characteristic of chlorite. There were other X-ray reflections present that possibly could be indexed as odd orders of a 14 Å basal reflection, however, so that further study was warranted.

Single crystal X-ray study reveals that there is a 14 Å reflection, but that it is very weak and is difficult to resolve from the white radiation background. Of the first thirty orders of the 14 Å basal reflection, only 0.0.9, 0.0.11, and 0.0.15 could not be detected. Heating a powdered specimen at 500 °C for one hour or more produces an intense 14 Å reflection with a spacing that is only slightly smaller than the unheated value of 14·21 Å determined from single crystal study. Thus, the specimen is a Ni-rich chlorite (nickelian clinochlore) that is unique in the virtual absence of a 14 Å reflection.

All twenty-five crystals examined by precession photography are twinned by the mica law and have a mosaic texture such that a detailed structural refinement is not feasible. By comparison with the calculated structure amplitudes listed by Bailey and Brown (1962), the chlorite layer-interlayer units can be identified as the I*a* structural type. The end-member nickel chlorite (nimite) described from Barberton, South Africa, by de Waal (1970) is of the more common II*b* structural type. Brindley and de Souza (1975) also have described I*a* Ni-chlorites in laterites from Brazil, but their specimens contain only 5·5 to 8·0% NiO in contrast to the 14·6% NiO of the Western Australian specimen.

Comparison of the intensities of o*kl* reflections on precession and Weissenberg photographs with those calculated for several 2-layer stacking sequences of I*a* layers derived by Mathieson and Walker (1954) served to identify the Western Australian chlorite as the *s* type. In this stacking arrangement the $a/3$ shift within each 2:1 layer is always along $-X_1$ (*L* layers in the terminology of Brindley *et al.*, 1950), the interlayer sheet has the I*a* orientation, and successive 2:1 layers alternately are shifted by $+b/3$ and $-b/3$ along the *Y* axis to create the 2-layer periodicity. Shirozu and Bailey (1966) and de la Calle *et al.* (1976) have shown that the *s* structure is probably the most stable arrangement of layers for vermiculite. This chlorite should weather to vermiculite with a minimum of structural change, therefore, and golden-yellow flakes present in the drill cuttings do prove to be Ni-vermiculite.

The powder pattern of the nickelian chlinochlore indexed on the basis of the 2-layer cell is listed in Table I. The ratio of 9·0 for the 0.0.6:0.0.10 intensities (for a 2-layer cell) is very high and indicates such a large concentration of octahedral heavy elements in the interlayer sheet relative to the 2:1 layer that it is at the very end of the scale on the determinative chart of Petruk (1964) with a degree of asymmetry near −2·0. Because the octahedral sheets in the 2:1 layer and in the interlayer are separated along *Z* by $c/2$, the scattered contributions from the two sheets are exactly in-phase for even orders of o*o*l, assuming a 1-layer cell, and out-of-phase for odd orders. The odd-order *F* values then are entirely due to the contributions of the tetrahedral sheets for cases of equal scattering power in the two octahedral sheets. For asymmetric distributions of octahedral scattering power, as in this chlorite, the odd-order *F* values have an added

TABLE I. *Indexed powder pattern*

hkl	*Int.*	d_{obs}	d_{calc}	*hkl*	*Int.*	d_{obs}	d_{calc}
002	1	14·20	14·213	13.14	5	1·569	1·569
004	100	7·111	7·107	20.$\bar{16}$			1·569
006	55	4·740	4·738	060	50	1·543	1·545
02.*l*	10	4·605	4·634	33$\bar{2}$			1·543
11.*l*			4·604	064	30	1·508	1·509
008	60	3·556	3·553	33$\bar{6}$			1·508
00.10	6	2·845	2·843	332			1·508
13$\bar{2}$	40	2·652	2·654	066	15	1·469	1·469
200			2·652	33$\bar{8}$			1·468
132	15 B	2·593	2·594	334			1·468
20$\bar{4}$			2·593				
13$\bar{4}$	30 B	2·552	2·552	00.20	20	1·417	1·421
202			2·550	068			1·417
				33.$\bar{10}$			1·416
13$\bar{6}$	50	2·390	2·391	336			1·416
204			2·389	13.$\bar{18}$	2	1·398	1·398
136	20	2·264	2·266	20.16			1·398
20$\bar{8}$			2·265	260	20B	1·333	1·335
13$\bar{8}$	2	2·201	2·202	40$\bar{4}$			1·334
206			2·200	13.18		1·324	1·323
00.14	10 B	2·027	2·030	20.$\bar{20}$			1·323
13.$\bar{10}$	30 B	2·009	2·010	264	25	1·295	1·297
208			2·009	40$\bar{8}$			1·296
				06.12			1·294
13.10	5	1·887	1·888	33.$\bar{14}$			1·293
20.$\bar{12}$			1·887	33.10			1·293
13.$\bar{12}$	2	1·830	1·830				
20.10			1·829	26$\bar{8}$	2	1·275	1·276
15.*l*	5	1·745	1·750	404			1·275
24.*l*			1·745	06.14	10B	1·226	1·229
31.*l*			1·737	33.$\bar{16}$			1·229
13.12	2	1·718	1·719	33.12			1·229
20.$\bar{14}$			1·719	268			1·225
13.$\bar{14}$	15	1·669	1·667	40.$\bar{12}$			1·224
20.12			1·667	00.24	10	1·184	1·185
				13.22	10B	1·132	1·136
				20.$\bar{24}$			1·135
				26.12			1·133
				40.$\bar{16}$			1·132

Pattern taken with Fe-$K\alpha$ radiation in 114·6 mm diameter camera. Intensities estimated visually. Indices such as 02.*l* indicate two-dimensional bands.

contribution that is a function of the difference in scattering power between the two octahedral sheets. Calculations for this specimen show that the magnitudes of the F values for the 00*l* reflections, including the virtual absence of the 14 Å reflection, can be explained quantitatively (Table II) by putting most of the available heavy elements in the interlayer sheet. The electron counts for octahedral cations in the interlayer and 2:1 sheets necessary for this calculation were determined by single crystal structural refinement.

The intensities of the 00*l* and 00$\bar{l}$ reflections for a crystal measuring 0·5 × 0·3 × 0·05 mm were recorded out to $2\theta = 97°$ with a Syntex $P2_1$ single crystal autodiffractometer in the variable-scan speed mode. Graphite monochromatized Mo-$K\alpha$ radiation was used, and only reflections for which $I > 2\sigma(I)$ were considered observed. The observed intensities were corrected for absorption empirically by comparing the 00*l* intensity data to complete Ψ scans (10° increments in Φ) for selected reflections collected at 2θ intervals of 10°. After correction for the Lorentz-

TABLE II. *Observed and calculated structure amplitudes of 00l reflections*

00.*l*	F_{obs}	F_{calc}	00.*l*	F_{obs}	F_{calc}	00.*l*	F_{obs}	F_{calc}
00·1	14·0	−16·6	00·11	—	4·6	00·21	10·4	−12·5
2	151·1	154·6	12	123·7	112·9	22	23·8	29·6
3	155·6	153·6	13	33·1	27·5	23	20·9	19·1
4	222·2	225·5	14	95·1	97·2	24	10·2	13·3
5	54·2	−48·9	15	—	1·8	25	4·9	−6·9
6	44·7	42·0	16	94·2	96·3	26	43·3	43·7
7	133·5	130·6	17	4·4	7·5	27	5·6	−3·3
8	35·6	26·8	18	17·2	19·2	28	14·5	13·5
9	—	2·9	19	34·4	37·3	29	12·4	9·1
10	133·6	137·7	20	24·6	27·3	30	21·4	16·6

Calculated values determined by least-squares refinement through variation of z/c co-ordinates, temperature factors, and cation multiplicities. Residual R_1 value equals 6·0%.

polarization factor, the results for 00*l* and 00$\bar{l}$ were averaged. Cell dimensions determined by least-squares refinement of fifteen high angle reflections are $a = 5{\cdot}346(2)$, $b = 9{\cdot}268(3)$, $c = 28{\cdot}649(9)$ Å, and $\beta = 97{\cdot}10(4)°$.

A one-dimensional electron-density projection on to Z computed at 3° intervals from $2\pi z/c = 0°$ to 180°, equivalent to fractional coordinates from 0 to 0·5, and utilizing the observed F values of Table II confirms the greater concentration of octahedral scattering power in the interlayer sheet at $2\pi z/c = 0°$ than in the 2:1 octahedral sheet at 180° (fig. 1). Integration of the octahedral peak densities in fig. 1 and least-squares refinement of the one-dimensional structure both yield electron counts near 64·5 per formula unit in the interlayer and 43·8 in the 2:1 layer. The peak for the interlayer OH plane at $2\pi z/c = 25{\cdot}5°$ in fig. 1 is lower than that for the other anion planes and suggests that there are vacancies at this level. Correspondence of the observed

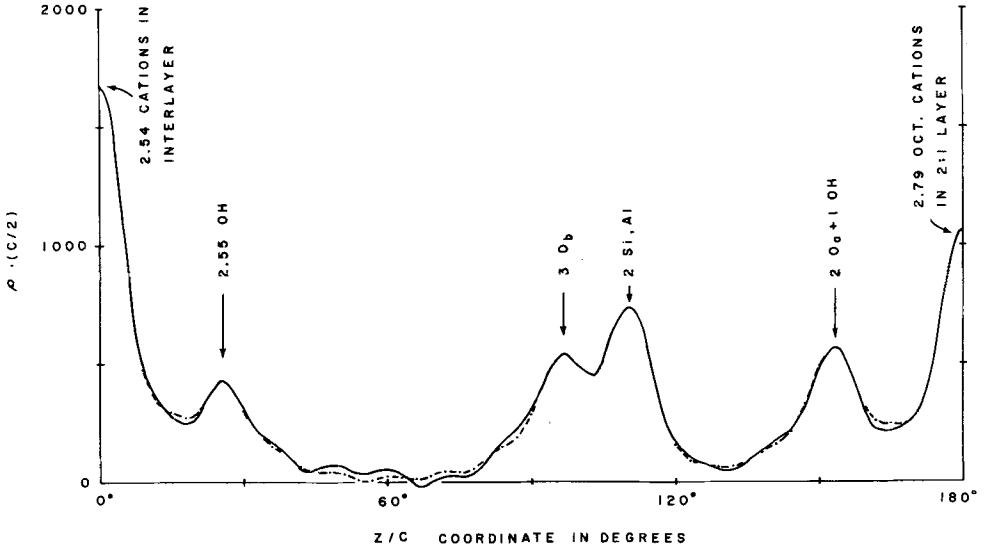

FIG. 1. One-dimentional electron-density projection on to Z. Observed density in solid line, calculated density in dashed line. The cation totals listed for the interlayer and the 2:1 layer are not unique and refer to the solution cited in the text.

and calculated electron densities in fig. 1 was achieved only by assuming 15% vacancies for the interlayer OH plane. Because the original analysis (Riley, 1975) was allocated on the basis of a full complement of anions, the composition has been recalculated on the assumption of 27·1 positive charges per formula unit. This yields $(Mg_{1\cdot98}Ni_{1\cdot22}Fe^{3+}_{1\cdot08}Fe^{2+}_{0\cdot67}Al_{0\cdot30}Ti_{0\cdot08}\square_{0\cdot67})(Si_{2\cdot93}Al_{1\cdot07})O_{10}(OH)_{7\cdot1}$. The total electron count for this octahedral composition is 103, assuming 50% ionization, rather than the experimental value of 108. This is a reasonable fit in view of the experimental errors involved and the uncertainty of the assumptions as to allocation basis and degree of ionization.

Two restrictions govern the compositions of the two octahedral sheets: first, the cations in the interlayer should contain 20 ± 5 more electrons than the cations in the 2:1 octahedral sheet with a resulting degree of asymmetry of heavy cations near $-2{\cdot}0$; secondly, the interlayer must carry a substantial net positive charge, as is the case in all chlorites. These restrictions require that virtually all of the Fe^{3+} and most of the Ni and Fe^{2+} be concentrated in the interlayer sheet. Although it is not possible to give a unique solution, a reasonable solution that agrees with the over-all composition and that satisfies the two conditions above gives $(Ni_{1\cdot0}Fe^{3+}_{1\cdot08}Fe^{2+}_{0\cdot38}Ti_{0\cdot08}\square_{0\cdot46})$ for the interlayer and $(Ni_{0\cdot22}Fe^{2+}_{0\cdot29}Mg_{1\cdot98}Al_{0\cdot30}\square_{0\cdot21})$ for the 2:1 layer. The high concentration of Fe^{3+} in the interlayer coupled with the defect anion planes suggest that partial oxidation and dehydration of the interlayer may have occurred.

Acknowledgements. Acknowledgement is made to the donors of the Petroleum Research Fund, administered by the American Chemical Society, for partial support of this research by grant 8425-AC2 and to the National Science Foundation for partial support through grant EAR76-06620. Publication is by permission of Carpentaria Exploration Co. Pty. Ltd. and Mount Isa Mines Ltd.

Department of Geology and Geophysics S. W. BAILEY
University of Wisconsin-Madison
Madison, Wisconsin 53706, U.S.A.

Technical Services Department JOHN F. RILEY
Mount Isa Mines Limited
Mount Isa, Queensland 4825, Australia

REFERENCES

Bailey (S. W.) and Brown (B. E.), 1962. *Am. Mineral.* **47,** 819–50.
Brindley (G. W.) and De Souza (J. V.), 1975. *Mineral. Mag.* **40,** 141–52.
—— Oughton (B. M.), and Robinson (K.), 1950. *Acta Cryst.* **3,** 408–16.
De La Calle (C.), Dubernat (J.), Suquet (H.), Pezerat (H.), Gaultier (J.), and Mamy (J.), 1976. *Proc. Internat. Clay Conf., Mexico City,* 201–9.
De Waal (S.), 1970. *Am. Mineral.* **55,** 18–30.
Mathieson (A. McL.) and Walker (G. F.), 1954. Ibid. **39,** 231–55.
Petruk (W.), 1964. Ibid. **49,** 61–71.
Riley (J. F.), 1975. *Mineral. Mag.* **40,** 200–2.
Shirozu (H.) and Bailey (S. W.), 1966. *Am. Mineral.* **51,** 1124–43.

[*Manuscript received 13 December 1976, revised 26 April 1977*]